ASTRONOMY & ASTROPHYSICS
SUPPLEMENT SERIES

Astron. Astrophys. Suppl. Ser. **136**, 173–177 (1999)

ASCA observations of massive medium-distant clusters of galaxies

I. A 1300 and A 1732⋆

M. Pierre[1], H. Matsumoto[2,3], T. Tsuru[2], H. Ebeling[4], and R. Hunstead[5]

[1] CEA/DSM/DAPNIA, Service d'Astrophysique, F-91191 Gif-sur-Yvette, France
[2] Department of Physics, Faculty of Science, Kyoto University, Sakyo-ku, Kyoto 606-8502, Japan
[3] Cosmic Radiation Laboratory, RIKEN, 2-1 Hirosawa, Wako, Saitama 351-0198, Japan
[4] Institute for Astronomy, University of Hawaii, 2680 Woodlawn Dr., Honolulu HI 9622, U.S.A.
[5] School of Physics, University of Sydney, NSW 2006, Australia

Received August 31, 1998; accepted January 7, 1999

Abstract. We have selected a sample of 10 medium distant ($z \sim 0.1 - 0.3$) clusters for deep, high-resolution, multi-wavelength observations in order to investigate in detail their dynamical state. This paper presents the analysis of the ASCA data for the two sample clusters observed under the ESA time allocation. For A 1300 and A 1732 we find temperatures and metal abundances for the intra-cluster medium of $kT = 11$ keV, $Z = 0.2$ and $kT = 6$ keV, $Z = 0.3$ respectively.

Key words: galaxies: clusters: general; A 1300; A 1732 — intergalactic medium — X-rays: galaxies

1. Introduction

Massive clusters of galaxies are fundamental cosmological probes because their formation rate — and formation history — depends strongly on both the value of Ω and the type of dark matter assumed. It is therefore of prime interest to detect and study very massive distant clusters. However, the detailed analysis of cluster properties (dynamics, virialization stage, galaxy content, ICM enrichment, etc.) requires large amounts of observing time and, beyond $z \sim 0.5$, is strongly limited by the angular resolving power of present-day instruments. As a result, the $0.2 < z < 0.3$ interval offers at present the best compromise for obtaining detailed multi-wavelength data for a statistically significant set of distant clusters. In this context, we have selected 10 medium distant, X-ray bright (i.e., massive) systems from a ROSAT All-Sky Survey flux limited sample of ~ 40 clusters located in the Hydra region (Pierre et al. 1994a).

Table 1. The cluster sample

ROSAT ID	Abell ID	redshift
RX J1023.8−2715	Abell 3444	0.255
RX J1031.6−2607		0.247
RX J1050.5−0236	Abell 1111	0.165
RX J1046.8−2535		0.243
RX J1103.6−2329		0.187
RX J1131.9−1955	Abell 1300	0.307
RX J1203.2−2131	Abell 1451	0.199
RX J1314.5−2517		0.244
RX J1315.0−4236		0.105
RX J1325.1−2013	Abell 1732	0.192

Note that, according to the RASS, these objects all have a luminosity $\geq 5\ 10^{44}$ erg s^{-1}. However, our subsequent deep HRI pointings have revealed that some are contaminated by a point-like source — i.e., an AGN — which is supported by the presence of a strong radio source at the cluster center. This will be discussed in detail by Lémonon et al. (1998).

For this sub-sample (Table 1), we undertook deep optical (CFHT, NTT), X-ray (ROSAT, ASCA), radio (AT) and infrared observations (ISO) (Pierre et al. 1994b). This unique database will yield insights into the formation processes of both clusters and galaxies, processes which are very likely to be intimately related. In this context, a general — and crucial — point is the evolution of the dynamical state of clusters. In hierarchical CDM-type scenarios, clusters are believed to form continuously, but not necessarily at the same rate. Indeed, using a power ratio technique applied to clusters extracted from classical CDM simulations, Tsai & Buote (1996) find that there is a continuous competition between relaxation and formation rates throughout the whole cluster history. They do

Send offprint requests to: M. Pierre (mpierre@cea.fr)

⋆ Paper based on observations obtained in the course of the ESA/ISAS Guest Investigator Programme.

Table 2. Cluster data

Cluster	z	σ_v km s^{-1}	L_X [0.1–2.4] 10^{44} erg s^{-1}	N_H 10^{20} cm^{-2}
A 1300	0.307	1200	18 (PSPC)	4.5
A 1732	0.193	1100	9.2 (HRI)	7.8

Velocity dispersions and luminosities are from Lémonon et al. (1999). N_H is a $\lambda 21$ cm value from Dickey & Lockman (1990).

not observe a significant change from high redshifts until $z \sim 0.6$, where both effects come into balance; at more recent times the formation rate levels off. Focusing on the very inner cluster regions (a few tens of kpc), the influence of the central galaxy appears to be responsible for the disturbed X-ray structure often observed, this region being more or less isolated from the rest of the cluster. Also, isophote morphologies derived from deep ROSAT HRI pointings suggest that below $z \sim 0.1$ the outer parts of clusters are less disturbed than in the $0.1 - 0.3$ redshift range (Pierre & Starck 1998).

As time goes on, cluster masses increase through matter accretion along filaments and, consequently, potential wells deepen. The merging process, however, takes time to produce relaxed systems. It is therefore of major interest to study cluster X-ray temperatures, together with optical data and X-ray morphologies, since the ICM temperature may not only reflect the depth of the gravitational potential but also contain the signature of recent mergers. This has been investigated at low redshift with detailed temperature maps (e.g., Briel & Henry 1996). For distant clusters where spatially resolved X-ray spectroscopy is not possible, deviations from the well known correlations (L_X, T_X, metallicity) can give an indication of the degree of cluster relaxation.

We present here the first two ASCA observations of our sample clusters, obtained under the ESA/ISAS time allocation; ASCA observations of the remaining eight clusters, performed under ISAS time, will be presented in a forthcoming paper (Matsumoto et al. 1999, in preparation). General information about the two clusters is given in Table 2. A 1300 is very luminous in the X-ray band. Both optical and ROSAT PSPC observations indicate that the cluster is in a recent post-merging phase (Lémonon et al. 1997). This is corroborated by the presence of a radio halo at the cluster center (Reid et al. 1999), a rare phenomenon at this redshift, but one increasingly associated with mergers.

ISOCAM observations of A 1732 revealed that the IR emitting galaxies tend to avoid the cluster center and are most likely due to galaxy interactions (Pierre et al. 1996). For A 1300, we find the ISO galaxies to be some 50% more luminous at 15 μm than in our other sample clusters; this may be interpreted in terms of enhanced star formation associated with the merger (Lémonon et al. 1999).

Throughout the paper we assume $H_0 = 50$ km s^{-1} Mpc^{-1} and $q_0 = 1/2$.

2. Observations and data reduction

Table 3 summarizes the ASCA observations. The GIS data were obtained with the normal PH mode, and the SIS data using the BRIGHT2 1 CCD mode. The targets were centered at the nominal position of the 1 CCD mode, which causes a slight position offset on the GIS images. All the subsequent analysis has been carried out with the XSPEC_8.5 and FTOOLS_3.5 packages using the screened data provided by the ASCA Standard Analysis from NASA/GSFC.

The ROSAT images of A 1300 and A 1732, filtered by a wavelet multi-resolution algorithm with a rigorous treatment of photon noise (Starck & Pierre 1998), are shown in Lémonon et al. (1997) and Pierre et al. (1996) respectively. At the ASCA angular resolution, A 1732 does not show significant structure as already inferred from the 30 ks HRI pointing which revealed a very regular morphology and a moderate cooling flow of $\sim 200\ M_\odot$/year. A 1300, on the other hand, is clearly elongated, in good agreement with the PSPC observation that was used to infer the post-merger state of the cluster; no HRI image is available for this cluster.

An elliptical region has been selected for extracting the SIS/GIS spectra of A 1300 and an circular region for A 1732; this is shown in Fig. 1 and Fig. 2. For both objects, the background area was selected in the vicinity of the source but excluding the cluster outskirts (beyond $8'$ from the source center). In an attempt to improve signal-to-noise, we have also used background spectra from blank-sky fields, since both clusters are in the direction of moderate N_H. This did not lead to a significant improvement in the spectral fit accuracy (see Table 4). Note, also, that blank-sky observations are presently available only for the GIS detector and not for the SIS in the BRIGHT2 1 CCD mode.

In addition, we made use of our 8.6 ks ROSAT PSPC observation of A 1300 to complement the spectral analysis.

3. Spectral analysis

After extraction, all spectra were rebinned requiring a minimum of 20 and 30 counts per bin and selecting energy channels in the ranges $0.7 < E < 10$ keV and $0.5 < E < 10$ keV for the GIS and SIS spectra respectively. We fitted a Raymond-Smith spectrum attenuated by photoelectric absorption from the Galaxy, the only fixed parameter being the cluster redshifts. However, to allow for uncertainties in the calibration of the different instruments, the normalizing constants were fitted independently for each instrument. The spectra are presented

Table 3. Journal of observations

Target	Date	Exposure (ks) & Countrate (c/s)			
		SIS0	SIS1	GIS2	GIS3
A 1300	1996 June	41.2 0.15	41.1 0.13	43.4 0.099	43.4 0.13
A 1732	1997 July	44.6 0.14	44.1 0.12	46.4 0.093	46.3 0.12

The countrates have been integrated within a radius of $500''$ in the $[0.7-10]$ keV band for the GIS images and within a radius of $250''$ in the $[0.4-10]$ keV band for the SIS.

Table 4. Results from the spectral analysis; errors are given for a 90% confidence interval. Rest frame absorption corrected luminosities have been calculated from the GIS countrate using the temperatures and metallicities obtained by ASCA (this table) and $N_{\rm H}$ values listed in Table 2

	T keV	$N_{\rm H}$ 10^{20} cm^{-2}	Abund. Z	Red. χ^2	$L_{\rm X}$ [2–10], $L_{\rm X}$ $[0.1-2.4]$, $L_{\rm Bol}$ 10^{44} erg s^{-1}
A1300					30, 21, 68
GIS2+GIS3	$9.7^{+1.8}_{-1.3}$	$7.3^{+5.1}_{-4.7}$	$0.12^{+0.13}_{-0.12}$	1.00	
GIS2+GIS3+PSPC	$10.4^{+1.3}_{-1.2}$	$4.4^{+0.7}_{-0.6}$	$0.12^{+0.14}_{-0.12}$	1.06	
SIS0+SIS1+GIS2+GIS3+PSPC	$11.4^{+1.4}_{-1.0}$	$4.6^{+0.8}_{-0.6}$	$0.16^{+0.12}_{-0.12}$	1.12	
SIS0+SIS1+GIS2*+GIS3*+PSPC	$11.4^{+1.3}_{-1.0}$	$4.6^{+0.9}_{-0.6}$	$0.17^{+0.11}_{-0.12}$	1.12	
A1732					9.4, 9.3, 20
GIS2+GIS3	$5.6^{+0.7}_{-0.6}$	$11.8^{+5.0}_{-5.0}$	$0.31^{+0.13}_{-0.11}$	1.05	
SIS0+SIS1+GIS2+GIS3	$5.5^{+0.4}_{-0.4}$	$14.7^{+2.3}_{-2.3}$	$0.30^{+0.08}_{-0.08}$	0.97	
SIS0+SIS1+GIS2*+GIS3*	$5.5^{+0.4}_{-0.3}$	$14.7^{+2.3}_{-2.2}$	$0.29^{+0.09}_{-0.07}$	0.97	

* Indicates that the GIS spectra were extracted using a background from blank-sky observations, otherwise the background has been routinely estimated from our images using regions free of sources.

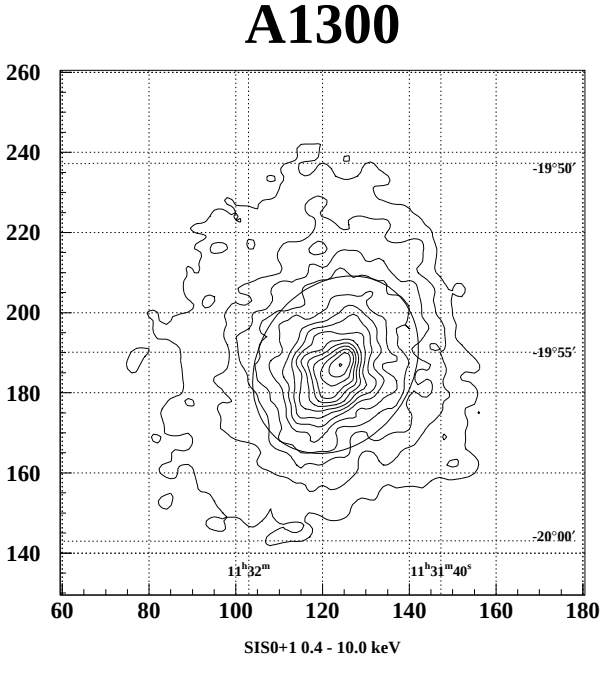

Fig. 1. SIS image of A 1300 in the $[0.4-10]$ keV band. The pixel size is $6.3''$ and the image has been filtered by a Gaussian having a σ of 1.5 pixel. Contours levels are 1.0, 2.0, 3.0... counts/pixel. The region extracted for the spectrum is indicated by an ellipse

in Figs. 3 and 4 and results from the spectral fitting summarized in Table 4.

The hydrogen column density is poorly constrained by the ASCA detectors in the low energy range. However, when the PSPC data for A 1300 are added in, the agreement with the radio measurement is excellent.

Luminosities (Table 4) were calculated by circular integration on the GIS images within a radius of $\sim 500''$ corresponding to 2.8 Mpc for A 1300 and 2.1 Mpc for A 1732. We used temperatures and abundances determined from the spectral analysis whereas $N_{\rm H}$ was fixed at its radio value. The agreement with the ROSAT measurements (Table 2) is excellent for A 1732. For A 1300, the PSPC measurement is about 15% lower than the ASCA one; this can be readily understood as the PSPC luminosity has been calculated from the fitted King profile, whereas the ASCA luminosity, obtained by simple circular integration, is probably contaminated by unresolved point sources conspicuous in the PSPC image.

4. Discussion and conclusions

For A 1300 we have measured the temperature in two concentric regions, divided so as to give comparable numbers of source photons: an inner circle of size comparable with that of the PSF (radius $3'$) and the surrounding annulus. Both sub-regions show temperatures compatible with

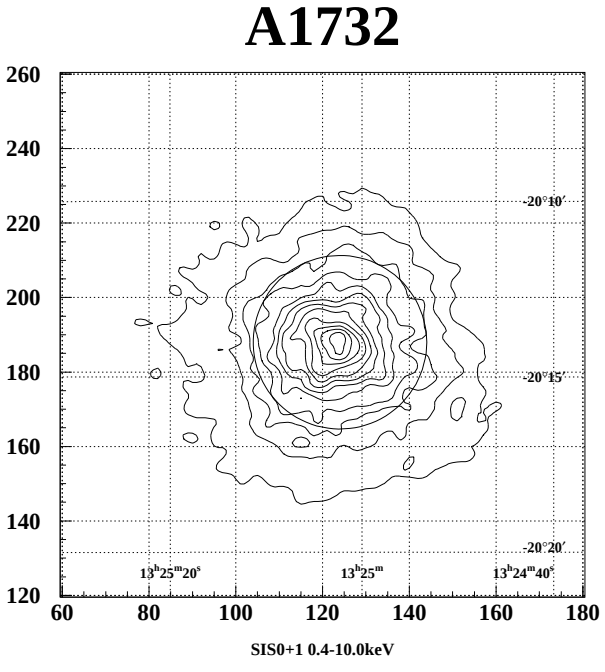

Fig. 2. SIS image of A 1732; otherwise as for Fig. 1

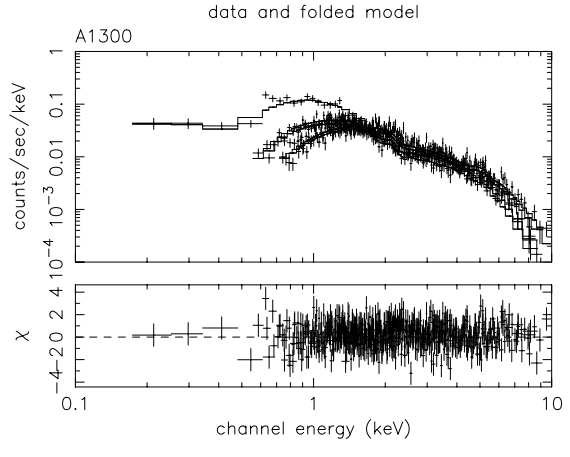

Fig. 3. *Upper panel*: Individual SIS0, SIS1, GIS2, GIS3 and PSPC spectra of A 1300, together with the best fitting model. *Lower panel*: Residual (observed − fitted) spectrum

the whole region, but with larger uncertainties. Thus, the question of a temperature gradient in A 1300, as suggested by the PSPC observation, remains open, since the cluster is not well resolved by ASCA and its flux is too weak to attempt any spatial/energy deconvolution.

We have also investigated the presence of a power-law contribution to the X-ray emission from A 1300, possibly associated with the radio halo. The spectral fitting, however, did not yield any conclusive results (no improvement in χ^2) nor a useful limit to such a non-thermal contribution.

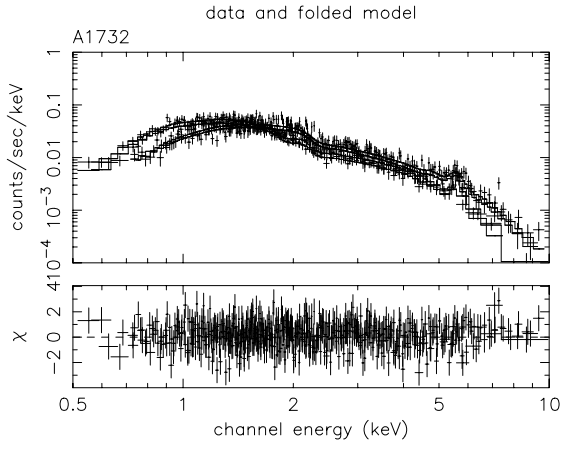

Fig. 4. *Upper panel*: Individual SIS0, SIS1, GIS2 and GIS3 spectra of A 1732, together with the best fitting model. *Lower panel*: Residual (observed − fitted) spectrum

A 1300 has rather a low metal abundance ($\sim 0.17 \pm 0.1$ solar). This, taken with its high temperature and luminosity, fits well into the post-merger picture sketched by Lémonon et al. (1997). The cluster was shown to be quite extended with a flat luminosity distribution — suggesting that the merging entities have not yet reached the state of a virialized cluster — and thus, the elapsed time has been too short for a cooling flow to form. This is in agreement with Allen & Fabian (1998) showing that high z non-cooling flow clusters tend to have lower metallicities (~ 0.2) than cooling flow clusters.

Mushotzky & Scharf (1997) and Tsuru (1998) have shown that there is no significant change in the $L_{\rm XBol} - T_{\rm X}$ relation out to $z \sim 0.4-0.6$ and our present data points are well within the overall distribution. A similar agreement (within 2 sigma of the mean correlation) is also found between the Mushotzky & Scharf $\sigma_{\rm v} - T_{\rm X}$ correlation and our findings.

The ASCA analysis of A 1300 and A 1732 provides new data on medium-distant galaxy clusters. Their overall properties appear to follow the general trends, which show no evolution but a rather large scatter related to the various virialization stages present in the cluster population. In a forthcoming paper (Lémonon et al. 1999) we shall discuss in more detail the properties of these clusters and of their galaxy content in connection with observations in the infrared, optical and radio bands.

Acknowledgements. This work results from an ESA/ISAS collaboration based on the ASCA space programme. M.P. is grateful to the Centre National d'Études Spatiales for a "Sol et Espace" grant and enjoyed the hospitality at Kyoto University of the Cosmic Ray Group led by Pr. Koyama for two weeks in September 1997.

References

Allen S.W., Fabian A.C., 1998, MNRAS 297, L63-L68
Briel U.G., Henry J.P., 1996, ApJ 472, 131
Dickey J.M., Lockman F.J., 1990, ARA&A 28, 215
Lémonon L., Pierre M., Hunstead R., Reid A., Böhringer H., 1997, A&A 326, 34
Lémonon L., et al., 1999, A&A (in preparation)
Mushotzky R.F., Scharf C.A., 1997, ApJ 482, L13-L16
Pierre M., Böhringer H., Ebeling H., Voges W., Schuecker P., Cruddace R., MacGillivray H., 1994a, A&A 290, 725
Pierre M., Hunstead R., Reid A., et al., 1994b, ESO Messenger No. 78, 24
Pierre M., Aussel H., Altieri B., et al., 1996, A&A 315, L294
Pierre M., Starck J.-L., 1998, A&A 330, 801
Reid A., Hunstead R.W., Pierre M., 1999, MNRAS 302, 571
Starck J.L., Pierre M., 1998, A&AS 128, 397
Tsai J., Buote D., 1996, MNRAS 282, 77
Tsuru T.G., 1998, IAU Symp 188, Kyoto Aug. 1997, "The hot universe", Koyama, Kitamoto, Itoh (ed.), p. 65